A.A. KOSTEREV✉
Y.A. BAKHIRKIN
F.K. TITTEL

Ultrasensitive gas detection by quartz-enhanced photoacoustic spectroscopy in the fundamental molecular absorption bands region

Rice Quantum Institute, Rice University, Houston, TX 77251-1892, USA

ABSTRACT A trace gas sensor based on quartz-enhanced photoacoustic spectroscopy with a quantum cascade laser operating at 4.55 μm as an excitation source was developed. The sensor performance was evaluated for the detection of N_2O and CO. A noise-equivalent (1σ) sensitivity of 4 ppbv N_2O with 3 s response time to $(1 - 1/e)$ of the steady-state level was demonstrated. The influence of the relevant energy transfer processes on the detection limits was analyzed. Approaches to improve the current sensor performance are also discussed.

PACS 42.62.Fi; 43.35.Sx

1 Introduction

Quartz enhanced photoacoustic spectroscopy (QEPAS) first reported in 2002 [1] is a technique that potentially allows quantification of trace species in extremely small gas samples ($< 1\,mm^3$). This unique capability can be particularly useful in microbiological and entomological [2] studies. QEPAS is also suitable to be the basis of the portable gas sensors for field and industrial applications, because this technique has proved to be highly immune to environmental interference such as acoustic noise. The small size of the QEPAS absorption-sensing unit ($\sim 5\,mm$ typical dimensions) permits convenient integration with semiconductor laser sources such as laser diodes, quantum cascade (QC) and interband cascade (IC) lasers.

QEPAS was successfully applied to ammonia detection at $< 1\,ppm$ levels using a telecommunication DFB diode laser at 1.52 μm [3]. A number of other species such as H_2O, CO_2, C_2H_2 have also been detected using QEPAS with a widely tunable near-IR diode laser source (AltoWave3500, Intune Technologies) [4]. The best sensitivity to absorption achieved to date with QEPAS is $D(NH_3) = 7.2 \times 10^{-9}\,cm^{-1}W/\sqrt{Hz}$, as measured for ammonia at 50 Torr total pressure. Here D is determined as

$$D = \frac{\alpha_{\min} P}{\sqrt{\Delta f}} \qquad (1)$$

where $\alpha_{\min}$ is the absorption coefficient corresponding to the noise-equivalent signal, P is the optical excitation power and Δf is the detection bandwidth. D strongly depends on the energy transfer processes in the gas, which will be discussed in Sect. 3 in more detail. Variations of D however were found not to exceed a factor of two for the investigated optical transitions in the overtone region. Advances in quantum electronics provided equally powerful spectroscopic sources such as QC and IC lasers for the mid-IR region. The principal purpose of this work was to explore the applicability of QEPAS to the detection of different trace gas species in the mid-IR region of fundamental vibrational absorption bands. Since molecular absorptions in this region are typically ~ 100 times stronger than in the near-IR, concentrations ~ 1–10 ppb should be detectable if D does not change significantly. A QC laser operating at 4.55 μm was provided by Alpes Lasers [5].

The molecules selected for this study were N_2O and CO. Detection of trace concentrations of each of these species is of practical importance for a number of applications. N_2O is an important contributor to the global greenhouse effect [6–10]. Background concentration of nitrous oxide in the atmosphere ranges from 310 to 320 ppbv and increases with an average rate of 0.8 ppb/year [11].

CO constitutes the largest fraction of the pollutants found in industrial and urban atmospheres. It is produced primarily by the incomplete combustion of organic materials and also results from industrial processes and motor vehicles exhausts [12]. Background levels of CO found in relatively unpolluted air range from 0.2 to 1.0 ppmv [6, 12]. CO in exhaled human breath (400–300 ppbv) is an essential biomedical marker for noninvasive disease diagnostics in medicine [13].

2 Experimental details

A configuration of the laboratory QEPAS-based gas sensor is shown in Fig. 1. A continuous wave (cw), distributed feedback (DFB) QC laser was used as a photoacoustic excitation source. The laser was liquid nitrogen cooled and covered the spectral range of 2198.3–2195.5 cm^{-1} when its current was changed from the threshold at 317 mA to 650 mA. The laser radiation was collected with a 13 mm focal length aspherical lens L_1, positioned so that the source was imaged at 97 cm from the lens. Such a long refocusing distance re-

✉ Fax: +1-713/348-5686, E-mail: akoster@rice.edu
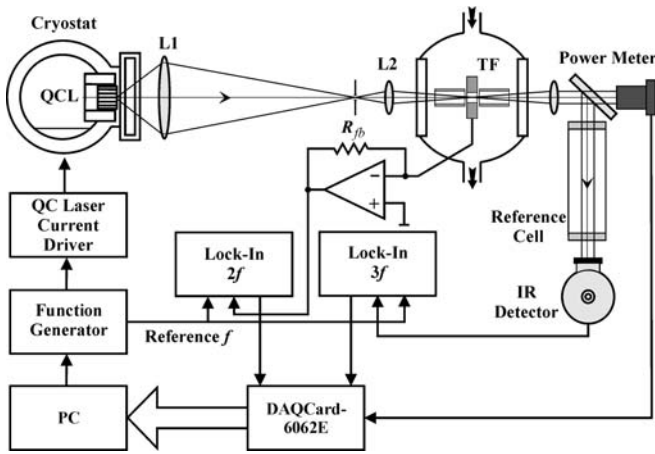
FIGURE 1 Schematic of the QEPAS trace gas sensor using a QC-DFB laser as an excitation source

duced the spherical aberration and allowed spatial filtering to be performed. A second lens L_2 (focal length 5 cm) re-imaged the source between the prongs of the quartz tuning fork (TF). An acoustic microresonator consisting of two fused silica tubes, each 2.45 mm long with a 0.32 mm inner diameter, was aligned perpendicular to the TF plane for sensitivity enhancement [1–4]. Care was taken to prevent the laser radiation from illuminating the microresonator walls. Such irradiation was found to result in a background photoacoustic signal because of radiation absorption in the microresonator silica tubes. The gas cell with $\sim 1\,\text{cm}^3$ volume containing the TF is described in further detail in [3]. The laser beam was recollimated upon exiting the TF cell. A beamsplitter was introduced to deflect a portion of the radiation to the IR detector, while most of the radiation passed to a power meter. A reference cell ($l = 13$ cm) was filled with a high concentration of the species under study (5%–10% peak absorption) for spectral reference.

The QC laser wavelength was modulated at a frequency $f = f_0/2$, where f_0 is the resonant frequency of the TF, and the detection of photoacoustic signal was performed at f_0, similar to [1–4]. The modulation was implemented by adding a sinusoidal component (typically ~ 4 mA peak-to-peak) on top of the dc laser current. The QEPAS experiments were carried out in two modes:

1. Scan mode. In this mode the dc component of the laser current was slowly tuned so that the central laser frequency swept over the desired spectral range.
2. Lock mode. The QC laser current was initially set to make the laser wavelength close to the absorption line center. The $3f$ component of IR detector signal A_{3f} was measured and a proportional correction to the dc component of the laser current $\Delta I = \text{const} \times A_{3f}$ was periodically made to maintain $A_{3f} = 0$. Thus, the laser wavelength was locked to the center of the targeted optical absorption line.

The TF generated piezoelectric current was converted to a voltage using a transimpedance amplifier with a feedback resistor $R_{\text{fb}} = 10\,\text{M}\Omega$. The outputs of the two lock-in amplifiers and other analog signals such as readings of pressure and gas flow meters were digitized using a PCMCIA data acquisition card (National Instruments DAQCard-6062E), which transferred the data to a notebook PC computer. LabView based

software provided computer control of the function generator (which in turn controlled the laser current) and the required data acquisition and processing.

Prior to each run of photoacoustic measurements the resonant frequency f_0 and Q-factor of the TF were determined. In order to do so, the ac voltage from the function generator was applied directly to the TF. The TF current was measured as a function of the applied voltage frequency. An example of the resonance curve is shown in Fig. 2. The parameters f_0 and Q depend on the gas pressure, major gas chemical composition, and the temperature. If the gas pressure and composition were maintained constant, the daily drift of f_0 did not exceed ± 0.02 Hz. The resonant curve allows the determination of the TF impedance as a ratio of voltage and current. The impedance is purely resistive at resonance, and its value R is related to the thermal noise of the TF:

$$\frac{\sqrt{\langle V_N^2 \rangle}}{\sqrt{\Delta f}} = R_{\text{fb}} \sqrt{\frac{4 k_B T}{R}} \tag{2}$$

where $\sqrt{\langle V_N^2 \rangle}$ is the RMS voltage noise observed at the transimpedance amplifier output, Δf is the detection bandwidth ($\Delta f = \frac{1}{2\pi\tau}$, where τ is the lock-in amplifier time constant), and T is the TF temperature. Other equivalent electrical parameters of the TF (L and C) can be found using the equations:

$$2\pi f_0 = \sqrt{\frac{1}{LC}}, \quad Q = \frac{1}{R}\sqrt{\frac{L}{C}} \tag{3}$$

Typically, the Q is 10 000 to 13 000 and $R \approx 90\,\text{k}\Omega$ in air or nitrogen at atmospheric pressure.

To detect the N_2O, P(30) transition of the ν_3 mode at $2195.633\,\text{cm}^{-1}$ was selected. CO detection was performed using its R(14) line at $2196.664\,\text{cm}^{-1}$ (the only CO absorption line within the tuning range of the available QC-DFB laser). The laser current required to reach each of these lines and the
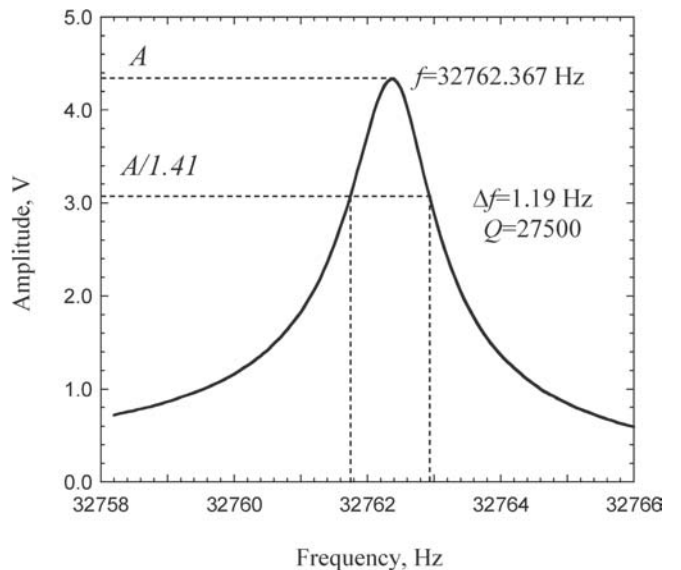
FIGURE 2 An example of the TF resonance curve. The TF current represented as the lock-in amplifier output is plotted versus frequency of the applied voltage sine wave. The TF is in air at 50 Torr pressure

corresponding laser power inside the TF cell were 590 mA (19 mW) and 493 mA (13 mW), respectively. The accessible CO line was ~ 2 times weaker in peak absorption than the N_2O line.

3   QEPAS and relaxation in gases

Generation of a photoacoustic wave involves the energy transfer from internal to translational molecular degrees of freedom. In the reported experiments a ro-vibrational state is initially excited, which is followed by a collision-induced V-T relaxation. If the vibrational energy excess directly relaxes into an unlimited bath of translational-rotational motions with a time constant τ (exponential population decay) and the laser input is modulated at a cyclic frequency $\omega = 2\pi f_0$, then the photoacoustic signal S is given by

$$S = S_0 \frac{1}{\sqrt{1 + \tan^2 \theta}}, \quad \tan \theta = \omega \tau_{VT}(C_{tr}/C_0) \qquad (4)$$

where S_0 is the photoacoustic signal for instant V-T transfer, τ_{VT} is the V-T relaxation time constant, θ is the phase shift between the excitation and photoacoustic signal, C_{tr} is the translational-rotational heat capacity at constant volume, and C_0 is the total heat capacity at constant volume [14]. If the relaxation is slow compared to the modulation rate ($\omega \tau_{VT} \gg 1$), then the photoacoustic sound generation is suppressed. Hence, the ability to detect a molecular species by means of PAS does not only depend on its optical absorption strength but is also influenced by the relaxation processes and the radiation modulation frequency.

The influence of relaxation processes on photoacoustic signal is negligible if $\omega\tau \ll 1$ condition is satisfied. Operating at a lower modulation frequency has the additional advantage of a higher photoacoustic signal even for fast-relaxing excited energy levels, because

$$S_0 = \text{const} \times E \frac{\alpha P Q}{f_0} \qquad (5)$$

where α is the absorption coefficient, P is the exciting radiation power, and E is a microresonator enhancement factor included in this equation to account for a particular QEPAS sensor design. However, the quartz tuning forks (TF) used as acoustic transducers in QEPAS so far are commercially available only at a resonant frequency of ~ 32.8 kHz (the modulation frequency in conventional PAS experiments does not usually exceed 4 kHz). Thus, for QEPAS $1/\omega \approx 5\,\mu s$ which is comparable to the V-T energy transfer rate in a number of gases and gas mixtures, especially below atmospheric pressure.

In traditional gas-filled resonator based PAS the detection sensitivity increases with pressure, because the resonator Q-factor and peak absorption both increase. The effect of pressure on detection sensitivity is different in QEPAS. Q and E were found to be higher at lower pressures, and according to (2), (3) and (5) the signal-to-noise-ratio, $SNR \sim E\sqrt{Q}$. At the same time α and relaxation rate are decreasing at reduced pressures. The wavelength modulation approach requires the modulation depth to match the absorption line width. Consequently, to determine the optimum conditions for trace gas

detection by means of QEPAS, the photoacoustic signal, S has to be mapped as a function of the host gas pressure and the laser modulation depth. In addition, for optimum performance the microresonator length must be adjusted so that its resonant frequency is equal to f_0 for the particular host gas composition.

4   Experimental results and discussion
4.1   *Nitrous oxide* (N₂O)

Nitrous oxide is present in ambient air at an almost constant (although location-specific) concentration of ~ 315 ppb, which is increasing at a 0.8 ppb/year rate [11]. This fact allowed us to use ambient air as a stable unlimited source of trace N_2O for QEPAS optimization. In order to promote the V-T relaxation of the laser-excited vibrational state of N_2O, sulfur hexafluoride (SF_6) was added to air in concentrations varying from 0 to 8% by volume. SF_6 has a high density of vibrational levels, that creates multiple options for resonant energy transfer in collisions with vibrationally excited molecules and a ladder for subsequent efficient multistep relaxation. Previously SF_6 was found to significantly improve the sensitivity of photoacoustic CO_2 detection as reported in [15]. Our measurements confirmed that the QEPAS signal following N_2O excitation is considerably larger in the presence of SF_6. Figure 3 shows the QEPAS signal detected at the absorption line center as a function of SF_6 concentration. Even a 0.5% addition of SF_6 resulted in 5.7 times signal enhancement. Too high (> 30%) percentage of SF_6 however caused the QEPAS signal to decrease for the following reasons:

1. Dilution of the air sample;
2. Detuning the microresonator resonance from f_0 due to the different speed of sound in SF_6 and N_2;
3. Increased thermal capacity of the carrier gas [$C_p(SF_6) = 97$ J/(mol K) and $C_p(N_2) = 29$ J/(mol K)]
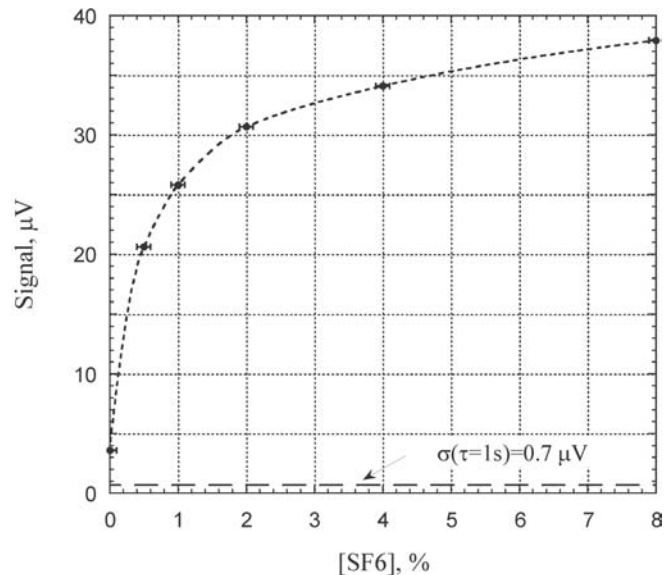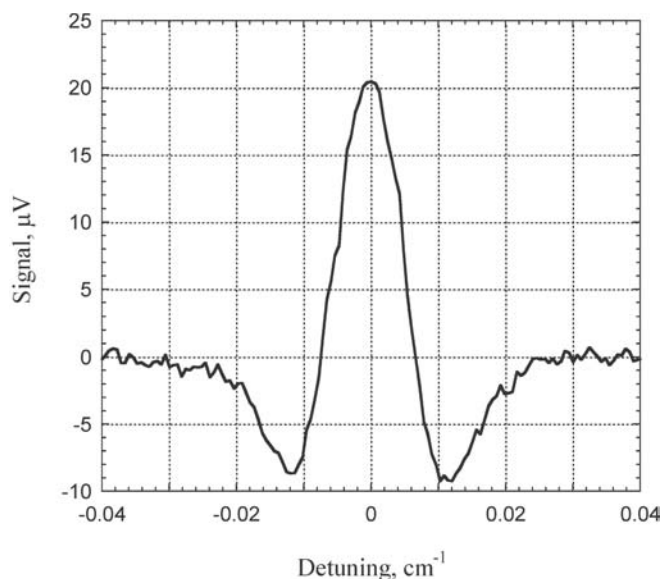

FIGURE 3   QEPAS signal of N_2O in ambient air (~ 315 ppb) as a function of added SF_6 concentration. Total gas pressure is 50 Torr and laser radiation power in the TF cell is 19 mW
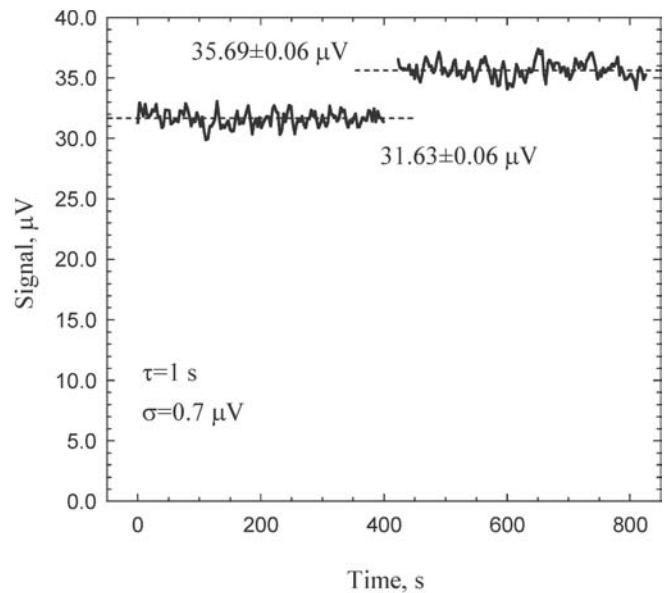
4. Decreased Q of the TF. At 50 Torr pressure the Q was observed to change from 26 600 in pure nitrogen to 10 800 in pure SF_6.

In this work a 5% SF_6 addition to sampled air was selected as optimum for most N_2O concentration measurements. Higher SF_6 concentration levels do not lead to a considerable gain in S but increase the SF_6 consumption and can cause sample contamination with impurities that may be present in SF_6. Such a SF_6 addition gives rise to a 9.8 times signal gain as compared to a N_2O signal from undoped air. The measurements were performed with a gas flow ranging from 50 to 70 standard cubic cm per minute (ccm; SF_6 was continuously added using a gas mixer) to avoid adsorption-desorption effects on the precision and accuracy of the experimental results. In Fig. 4 an example of QEPAS spectral data acquired for an ambient air sample with 5% SF_6 at a 50 Torr total pressure is shown. The lock-in amplifier time constant was set to 3 s, and the laser power in the TF cell was 11 mW. 50 Torr pressure was found to be optimum for N_2O detection in air or nitrogen.

A NOAA certified Nowat Ridge air sample from a cylinder filled in 1996 containing 313.3 ± 0.3 ppbv of N_2O (at the time of filling) was used for the QEPAS sensor calibration. A trace of the sensor readings for this sample (lock mode) followed by a trace for ambient air is shown in Fig. 5. In both cases 5% SF_6 was added. The lock-in amplifier time constant was set to $\tau = 1$ s and the measurements were repeated every 3 s. The laser power in the TF cell was 19 mW. The scatter of the results does not depend on the N_2O concentration or the laser power and is in agreement with the calculated thermal noise of the TF [16]. This calibration yields the sensor transfer function 0.101 μV/ppbv for N_2O, which in turn yields a room concentration $[N_2O] = 353.5$ ppb and a noise-equivalent detection sensitivity of 7 ppb for a 1 s time constant. The accuracy of the measured room $[N_2O]$ is deter-
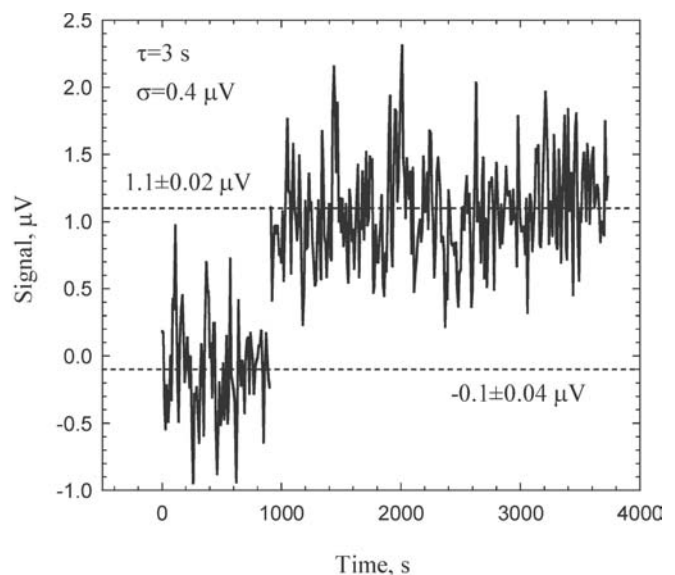

FIGURE 5   QEPAS signal in lock mode. *First part* (up to ~ 400 s): a sample of Niwot Ridge Colorado air supplied by NOAA in 1996; *second part*: ambient air

mined by the accuracy of the calibration gas data. A seemingly too high measured concentration of the N_2O in room air may indicate that some of the N_2O in the air sample collected in 1996 has decomposed. However, if we assume that the calibration is correct, the resulting inaccuracy will not exceed 15%.

Based on the above calibration, the N_2O concentration in a gas mixture containing ultrapure N_2 and 5% SF_6 (BOC Gases) was analyzed. The acquired data are presented in Fig. 6. For these measurements the lock-in time constant was increased to $\tau = 3$ s, which resulted in a noise reduction to

FIGURE 4   An example of the N_2O absorption line at 2195.633 cm^{-1} detected in ambient air at 50 Torr with QEPAS in a scan mode. Laser power in the TF cell is 11 mW, lock-in amplifier time constant is 3 s, and 5% SF_6 introduced to the air sample

FIGURE 6   QEPAS signal in lock mode. *First part* (up to ~ 1000 s): laser wavelength detuned from the absorption line; *second part*: laser is locked to the N_2O absorption line at 2195.633 cm^{-1}

0.4 μV, or a 4 ppb single measurement. The measurements were performed every 10 seconds. The initial portion of the plot (i.e. ∼ 1000 s) depicted in Fig. 6 shows the sensor readings when the laser wavelength was shifted off the absorption line (zero signal expected). A small deviation from zero is most probably due to the scattered laser light absorbed in the microresonator tube. The trace beyond 1000 s shows the sensor readings in the lock mode. The observed photoacoustic signal corresponds to 11 ppbv of N_2O in the analyzed gas.

The normalized QEPAS sensitivity $D(N_2O)$ based on the experiments reported above and the HITRAN database is $D(N_2O) = 1.5 \times 10^{-8}$ cm^{-1}W/$\sqrt{Hz}$. This number is ∼ two times higher (meaning lower sensitivity) than $D(NH_3)$ obtained in the near-IR region [3]. Two possible reasons for this are the slower V-T energy transfer in N_2O-N_2-5%SF_6 system and a shift of the microresonator resonance as a result of presence of SF_6 (E reduced in (5)). The potential relaxation pathways of the laser-excited N_2O energy level are shown in Fig. 7. When the P(30) line is excited, one rotational quantum (28 cm^{-1}) is removed from the molecular rotational energy. The first relaxation step is the distribution of this energy deficiency among rotational-translational (R,T) degrees of freedom, resulting in a *cooling* of the gas. Molecular collisions will also result in the following processes:

1. Energy transfer to the N_2 molecular vibration. This process can be of significant probability because of the close resonance between the N_2O ν_3 vibration (2223 cm^{-1}) and N_2 vibration (2331 cm^{-1}). Such energy transfers also result in gas *cooling* because the energy mismatch $\Delta E = -107$ cm^{-1} is borrowed from the bath of R,T motions.
2. Energy transfer to SF_6 vibrations. The dense manifold of SF_6 ro-vibrational levels ensures close resonance for some levels of SF_6 and N_2O, as well as facilitates the consequent V-T relaxation down the ladder of vibrational levels.
3. Energy transfer to other vibrational levels of N_2O, with the energy mismatch being released to (or absorbed from) the R,T degrees of freedom.
4. Following (1), N_2 excitation can be transferred to SF_6 molecules with a subsequent V-T relaxation of SF_6.

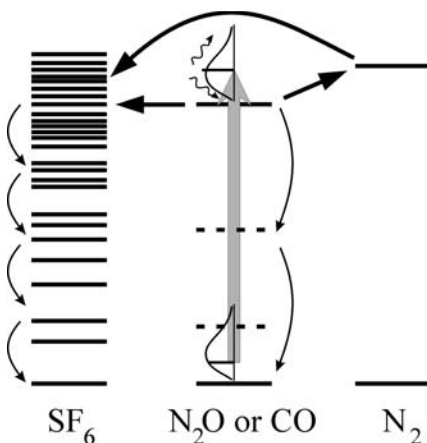**FIGURE 7**   Relaxation pathways following optical excitation (represented by wide gray arrow) of $v = 1$ level of N_2O or CO molecule

Relaxation of N_2 in dry air is known to be very slow [17]. Addition of 1% H_2O increases the relaxation rate 30 times, but even in this case and atmospheric pressure the relaxation time $\tau_{VT}(N_2) = 710$ μs and is much longer than $1/\omega = 5$ μs. Therefore, it is likely that some energy irreversibly leaks from N_2O to N_2 and becomes excluded from the photoacoustic signal generation (so-called ''kinetic cooling''). This process can contribute to the decrease in QEPAS sensitivity as compared to NH_3 near-IR detection along with a reduced Q-factor and microresonator resonance shift caused by SF_6 addition to the sampled gas.

4.2   *Carbon monoxide (CO)*

The QEPAS signal obtained with the excitation of the R(14) transition of CO molecules in N_2 as a host gas at 50 Torr total pressure was found to be 35 times weaker than the signal produced by an equally absorbing amount of N_2O in N_2:5%SF_6 [normalized to laser power: $D(CO) = D(N_2O)/35$]. Consequently, the QEPAS-based sensor was 70 times less sensitive to CO in terms of concentration than to N_2O. Unlike for N_2O detection, the addition of up to 10% of SF_6 did not result in a substantial sensitivity improvement. If the total pressure was increased up to 1 atm, the sensor response to CO followed the gradual decrease of the TF Q-factor. Thus, the single-measurement noise-equivalent sensitivity of QEPAS to CO at $\tau = 3$ s was 280 ppbv, which was not sufficient to monitor atmospheric CO.

Direct V-T energy transfer from vibrationally excited CO in a CO:N_2 mixture is known to be a slow process and can therefore be excluded from consideration on $1/\omega$ time scale. The fastest relaxation process following CO excitation is the rotational equilibration resulting in the release of 53 cm^{-1} [one rotational quantum for R(14) transition] of the total 2197 cm^{-1} per excited molecule. According to (4), the rotational equilibration will result in the photoacoustic signal with $\theta \approx 0$ and amplitude

$$S_R = S_0^i \frac{53 \text{ cm}^{-1}}{2197 \text{ cm}^{-1}} \approx S_0^i/40 \qquad (6)$$

Here S_0^i is a PAS signal that would be generated if all the absorbed optical energy is instantly released to translational motion of the gas molecules.

The next fastest process is the resonant energy transfer to N_2 molecules. The rate constant for this reaction was experimentally measured [18], and gives a relaxation time $\tau(CO-{}^{14}N_2) = 110$ μs if scaled to a 50 Torr pressure. Each reactive collision results in borrowing 187 cm^{-1} from the R,T bath to compensate for the energy mismatch, thus cooling down the gas. From (4) it follows that for this process $\tan \theta \approx 23$. The corresponding photoacoustic signal is

$$S_{CO-N_2O} = S_0^i \frac{187 \text{ cm}^{-1}}{2197 \text{ cm}^{-1}} \frac{1}{\sqrt{1+23^2}} \approx S_0^i/270 \qquad (7)$$

and is shifted in phase almost 90° with respect to S_R.

Consequently the net photoacoustic signal resulting from these two fastest energy transfer channels in a CO:N_2 mixture is practically equal to $S_R \approx S_0^i/40$. As $D(CO) = D(N_2O)/35$, we can conclude that:

1. N_2O V-T relaxation time in a N_2:5%S_6 host at 50 Torr $\tau(N_2O) < 0.6/\omega$ [i.e. $\tau(N_2O) < 3\,\mu s$], following from the condition that $\frac{1}{\sqrt{1+\tan^2\theta}} > \frac{35}{40}$;

2. the observed photoacoustic signal in a CO:N_2 mixture at 32.8 kHz is mostly the result of rotational relaxation. V-T energy transfer in this system is too slow to produce a measurable photoacoustic response at this modulation frequency.

5   Conclusions

This work demonstrated that the QEPAS technique can be successfully used for ultra-sensitive detection of trace gas species excited to $v = 1$ vibrational levels. The realized sensitivity to absorption $D(N_2O) = 1.5 \times 10^{-8}\,cm^{-1}W/\sqrt{Hz}$ allowed the detection of N_2O in air and nitrogen samples with a 4 ppbv noise-equivalent (1σ) sensitivity and 3 s response time to $(1 - 1/e)$ of the steady-state level. However, the results of our experiments indicate that V-T energy transfer from $v = 1$ excited level of simple molecules is slower than the relaxation of overtone vibrations [3, 4]. In some cases the relaxation rate can be enhanced by adding an appropriate species to the gas sample (e.g., SF_6 added to N_2 for N_2O detection). The vibrational relaxation of CO was found to be too slow to produce a measurable QEPAS signal. Nevertheless, we were able to detect this molecule with 280 ppbv noise-equivalent sensitivity due to the rotational relaxation related signal. Thus, a sensitivity improvement of only a few times (via higher laser power or by the means as discussed in the following paragraph) will make the QEPAS sensor reported in this work useful for atmospheric CO monitoring. SF_6 does not significantly promote vibrational deexcitation of CO, although it is efficient in case of N_2O. This suggests the involvement of lower vibrational levels of the N_2O molecule in V-T energy transfer.

We expect that refinement of the microresonator design and fabrication technology will lead to a considerable gain in QEPAS sensitivity. Future designs will minimize the openings at the junctions of the resonator tubes and TF, which will ensure better confinement of the photoacoustic sound waves. Another approach to better QEPAS detection sensitivity is to develop a custom-made TF with lower resonant frequency. The desired frequency shift can be achieved by adding compact weights to the ends of a standard 32.8 kHz TF. If this is done properly, only the parameter L will change in (3). It can be seen from (2), (3) and (5) that SNR will scale as $f_0^{-3/2}$. Thus, if the weights shift the TF frequency from 32.8 kHz to 10 kHz, the QEPAS sensitivity should theoretically increase 6 times, even if the V-T relaxation is instant.

REFERENCES

1 A.A. Kosterev, Y.A. Bakhirkin, R.F. Curl, F.K. Tittel: Opt. Lett. **27**, 1902 (2002)
2 F.G.C. Bijnen, F.J.M. Harren, J.H.P. Hackstein, J. Reuss: Appl. Opt. **35**, 5357 (1996)
3 A.A. Kosterev, F.K. Tittel: Ammonia detection using quartz-enhanced photoacoustic spectroscopy with a near-IR telecommunication diode laser, accepted for publication in Appl. Opt.
4 D. Weidmann, A.A. Kosterev, F.K. Tittel, N. Ryan, D. McDonald: Application of widely electrically-tunable diode laser to chemical gas sensing with quartz-enhanced photoacoustic spectroscopy, Opt. Lett. **29**, 1837 (2004)
5 A.A. Kosterev, Y.A. Bakhirkin, F.K. Tittel, S. Blaser, Y. Bonetti, L. Hvozdara: Appl. Phys. B **78**, 673 (2004)
6 D.C. Scott, R.L. Herman, C.R. Webster, R.D. May, G.J. Flesch, E.J. Moyer: Appl. Opt. **38**, 4609 (1999)
7 C.R. Webster, G.J. Flesch, D.C. Scott, J.E. Swanson, R.D. May, W.S. Woodward, C. Gmachl, F. Capasso, D.L. Sivco, J.N. Bailargeon, A.L. Hutchinson, A.Y. Cho: Appl. Opt. **40**, 321 (2001)
8 G. Wetzel, H. Oelhaf, R. Ruhnke, F. Friedl-Vallon, A. Kleinert, W. Kouker, G. Maucher, T. Reddmann, M. Seefeldner, M. Stowasser, O. Trieschmann, T. von Clarmann, H. Fischer: J. Geophys. Res. **107**(D16), 10.1029/2001JD000916 (2002)
9 M.H. Proffitt, K. Aikin, A.F. Tuck, J.J. Margitan, C.R. Webster, G.C. Toon, J.W. Elkins: J. Geophys. Res. **108**, 4110 (2003)
10 G. Kopp, H. Berg, T. Blumenstock, H. Fischer, F. Hase, G. Hochschild, M. Höpfner, W. Kouker, T. Reddmann, R. Ruhnke, U. Raffalski, Y. Kondo: J. Geophys. Res. **108**, 8308 (2003)
11 R.J. Martin: Nitrous oxide measurements in clean air, Proceedings of the Workshop on the Science of Atmospheric Trace Gases, ed. by T.S. Clarkson, NIWA Technical Report 15, p.115 (1998)
12 T. Holloway, H. Levy II, P. Kasibhatla: J. Geophys. Res. **105**, 12 123 (2000)
13 S.A. Kharitonov, P.J. Barnes: Am. J. Respirat. Critic. Care Med. **163**, 1693 (2001)
14 T.L. Cottrell, J.C. McCoubrey: *Molecular energy transfer in gases* (Butterworths, London 1961)
15 M. van Herpen: Continuous-wave optical parametric oscillator for trace gas detection in life sciences, Ph.D. Thesis, Katholieke Universiteit Nijmegen, Netherlands (2004) Chapt. 10
16 R.D. Grober, J. Acimovic, J. Schuck, D. Hessman, P.J. Kindlemann, J. Hespanha, A.S. Morse, K. Karrai, I. Tiemann, S. Manus: Rev. Sci. Instrum. **71**, 2776 (2000)
17 R.A. Rooth, A.J.L. Verhage, L.W. Wouters: Appl. Opt. **29**, 3643 (1990)
18 D.C. Allen, C.J.S.M. Simpson: Chem. Phys. **45**, 203 (1980)